Equidistant optimization of elliptical superconducting rf standing wave cavities

Valery Shemelin[1,*] and Vyacheslav Yakovlev[2]

[1]*Cornell Laboratory for Accelerator-based Sciences and Education (CLASSE), Ithaca, New York 14853, USA*

[2]*Fermi National Accelerator Laboratory, Batavia, Illinois 60510, USA*

(Received 17 July 2023; accepted 21 August 2023; published 5 September 2023)

A record accelerating rate was achieved earlier in standing wave (SW) SRF cavities when their shape was optimized for a lower peak surface magnetic field sacrificing the peak surface electric field. In view of new materials with higher limiting magnetic fields, expected for SRF cavities, in the first line of the Nb_3Sn, the approach to optimization of cavity shape should be revised. A method of equidistant optimization, offered earlier for traveling wave (TW) cavities is applied to SW cavities. It is shown here that without limitation by magnetic field, the maximal accelerating rate is defined not only by limitations of the electric field but to a significant degree by the cavity shape. For example, for a cavity with the aperture radius of $R_a = 35$ mm, the minimal ratio of the peak surface electric field to the accelerating rate is about $E_{\mathrm{pk}}/E_{\mathrm{acc}} = 1.54$. So, with the maximal surface field experimentally achieved $E_{\mathrm{pk}} \sim 125$ MV/m, the maximal achievable accelerating rate is about 80 MeV/m even if there are no restrictions by the magnetic field. Optimized cavity shapes with and without limitations by a magnetic field are presented. Another opportunity—optimization for a low magnetic field, is opening for the same material, Nb_3Sn, with the purpose of having a high quality factor and increased accelerating rate that can be used for industrial linacs with cryocooler-based cooling scheme.

DOI: 10.1103/PhysRevAccelBeams.26.092001

I. INTRODUCTION

A record accelerating rate was achieved earlier with elliptical SRF cavities [1] when their shape was optimized [2] so that the peak surface magnetic field B_{pk} was decreased by 10%, and the peak surface electric field E_{pk} was increased by 20% compared to the TESLA cavity with the same accelerating field E_{acc} on the cavity axis. This change of shape was done due to the understanding that the superheating field B_{sh} (170–250 mT for niobium according to different theoretical evaluations [3,4]) is the fundamental limit to acceleration in SRF cavities, and by decreasing the value of $B_{\mathrm{pk}}/E_{\mathrm{acc}}$, we can increase the accelerating rate E_{acc}. New materials, and first of all Nb_3Sn, are promised that they could be run at twice the magnetic field of Nb [4]. Does this mean that the accelerating rate can be twice the rate achieved in the Nb cavities? It seems that the surface electric field can become the next limit to the highest achievable accelerating rate. The surface electric field up to 125 MV/m has been demonstrated [1,5,6] in single-cell cavities. So, if this field is a limit, we need to decrease $E_{\mathrm{pk}}/E_{\mathrm{acc}}$ to achieve a maximal acceleration rate. For better results, as can be supposed, we should stay at equal distances from both limits. A method of equidistant optimization was offered earlier for TW cavities [7]. Now we apply this method to the SW elliptic cavities which are better studied than the TW SRF cavities and are easier in production than the TW ones. The presented study does not consider the influence of cavity shapes on higher order modes, which is the main criteria for certain applications, or on the multipactor threshold. However, as it was shown in [7], small deviations from the optimal shape can make the cavities multipactor-free without compromising the main figures of merit.

II. GEOMETRY OF AN ELLIPTICAL CAVITY

For an easier explanation of the following, let us remind the geometry of the cavities under consideration.

Contemporary superconducting rf cavities for high energy particle accelerators consist of a row of cells coupled together as shown in Fig. 1. The contour of a half-cell consists of two elliptic arcs and a straight segment tangential to both. The contour can be described by several geometrical parameters shown in Fig. 1(b). Three of these parameters, length of the half-cell L, aperture R_{a},

*vs65@cornell.edu

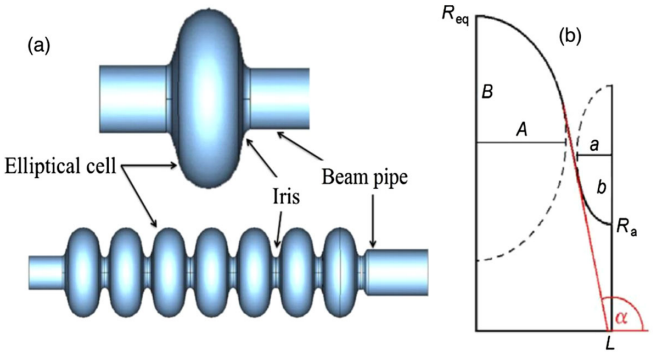

FIG. 1. (a) Single-cell and multicell elliptical cavities; (b) geometry of the half-cell.

and equatorial radius R_{eq} are defined by physical requirements: $L = \lambda/4$ (for π-mode, inner cells of a multicell cavity), where λ is the rf wavelength; the aperture is defined by requirements for coupling between cells and by the level of wakefields that can be allowed for a given accelerator; and the equatorial radius R_{eq} is used for tuning the cavity to a given frequency. The remaining four parameters (A, B, a, b) can fully describe the geometry. Here A, B and a, b are the half-axes of the equatorial and iris constitutive ellipses, respectively. The best combination of four parameters is the goal for the cavity shape optimization. The angle of the wall inclination between the axis of rotation and the straight segment of the wall is designated as α. The cavities with $\alpha < 90°$ are known as the reentrant cavities.

III. EQUIDISTANT APPROACH FOR OPTIMIZATON

Optimization of an elliptical cavity is usually done as a search for minimum B_{pk}/E_{acc} when the value of E_{pk}/E_{acc} is given. It is also possible to minimize E_{pk}/E_{acc} for a given B_{pk}/E_{acc} but the truth is that we need to reach as high of an accelerating gradient E_{acc} as possible before field emission or magnetic quench limits E_{acc} from increasing further. So, the ideal situation would be to reach both limits simultaneously using all the possibilities to increase E_{acc}. If we know the maximal achievable surface peak fields E^*_{pk} and B^*_{pk}, then the cavity having equal values of E_{pk}/E^*_{pk} and B_{pk}/B^*_{pk} will be at equal distances from either limit. Then the criterion of the shape optimization can be written as a minimum of the maximum of two values: E_{pk}/E^*_{pk} and B_{pk}/B^*_{pk}, or, shortly, min-max $(E_{pk}/E^*_{pk}, B_{pk}/B^*_{pk})$. We named this approach *the equidistant optimization*.

In the optimization, absolute values of E^*_{pk} and B^*_{pk} do not matter, only their ratio is important. This ratio depends on the geometry only. Values under the sign of min-max (see above) become equal in the result because E_{pk} and B_{pk} change reversely: when one of them increases, the other decreases, and vice versa.

The definition given above for the equidistant optimization can be rewritten in an equivalent form more convenient for calculations:

$$\begin{aligned} &\text{Goal} = \min E_{pk} \quad \text{if } E_{pk}/B_{pk} > E^*_{pk}/B^*_{pk} \quad \text{or} \\ &\text{Goal} = \min B_{pk} \quad \text{if } E_{pk}/B_{pk} < E^*_{pk}/B^*_{pk}, \end{aligned} \tag{1}$$

where the goal is a combination of the geometrical parameters A, B, a, and b, giving the desired minimum. The practice showed that the goals defined by the first or the second way differ by less than 0.01% if the accuracy of the geometrical parameters is 0.01 mm.

So, the cavity shape optimized for given values of E^*_{pk} and B^*_{pk} depends only on their ratio E^*_{pk}/B^*_{pk}; optimization, for example, for $E^*_{pk} = 120$ MV/m and $B^*_{pk} = 240$ mT will be the same as optimization for $E^*_{pk} = 100$ MV/m and $B^*_{pk} = 200$ mT. Let us call this optimization "optimization 100/200" just as a reminder that this ratio is for limiting surface fields of 100 MV/m and 200 mT, though a simple designation $\kappa = E^*_{pk}/B^*_{pk}$. equal in this case to 0.5 (MV/m)/mT also can be used.

Optimization for minimum B_{pk}/E_{acc} when the value of E_{pk}/E_{acc} is given can be revised in the light of the method proposed here. For example, well optimized for a given aperture, the TESLA cavity has $E_{pk}/E_{acc} = 2$ and $B_{pk}/E_{acc} = 4.2$ mT/(MV/m). If we assume that both limits, E_{pk} and B_{pk}, are achieved simultaneously in this optimization, then $E_{pk}/B_{pk} = E^*_{pk}/B^*_{pk} = 2/4.2$ (MV/m)/mT $= 100/210$ (MV/m)/mT. This means that this cavity can be treated as a cavity optimized for $E^*_{pk} = 100$ MV/m and $B^*_{pk} = 210$ mT, or, proportionally, for example, for $E^*_{pk} = 80$ MV/m and $B^*_{pk} = 168$ mT. The TESLA cavity cannot reach $E_{acc} > 50$ MV/m because in this case B^*_{pk} should be higher than 210 mT.

A possible future progress in the increase of achievable fields can change this proportion, as, for instance, done in [1]: a gradient of 59 MV/m was achieved in a single-cell reentrant cavity that corresponds to a peak surface electric field of 125 MV/m and a peak magnetic field of 206.5 mT. These values really look like maximal fields for existing cavities. The gradient was limited by a hard quench through the exponentially growing field emission when $E_{pk} > 100$ MV/m [5] shows that we are also close to the limit of the electric field. We can make another optimization with these parameters $125/206.5 \approx 120/200$, "optimization 120/200." If we knew what fields are maximum achievable, we would find the optimal shape from the first try. If we can afford the magnetic limiting field higher than 210 mT, but the limit in the electric field is still at the level of 125 MV/m, then for the accelerating rate higher than 62.5 MV/m, we should have $E_{pk}/E_{acc} < 2$.

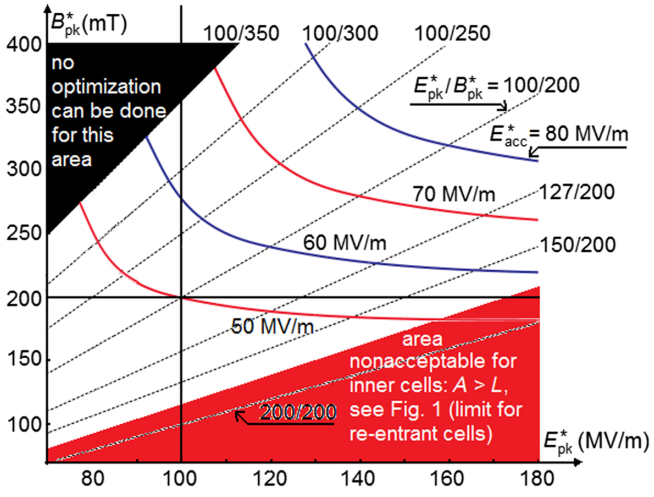

FIG. 2. Maximal achievable accelerating rates for different limiting electric and magnetic fields, $R_a = 35$ mm.

The difference between these two methods is in the fact that we do not know *a priori* what value of B_{pk}/E_{acc} we will have for a given value of E_{pk}/E_{acc} in the old method, but in the new method, we can choose the ratio between the extremal fields based on experiment and then perform the optimization.

Values of E_{pk}/E_{acc} and B_{pk}/E_{acc} will be obtained as a result of optimization when limiting fields are given. The procedure of optimization for min max $(E_{pk}/E^*_{pk}, B_{pk}/B^*_{pk})$ consists of a systematical change of the elliptical half axes A, B, a, and b (Fig. 1) decreasing maximal value in parentheses, as a result, both ratios become equal. This optimization method warrants a more complete study in comparison with the conventional method for SW cavity optimization.

IV. RESULTS OF OPTIMIZATION OF INNER CELLS

Optimization was done for the inner cell of a multicell cavity with the aperture radius $R_a = 35$ mm. The end cells and the single-cell cavities should be optimized separately because of the different boundary conditions at their ends. Besides, the end cells can be connected with beam pipes of different configurations (Fig. 1). We will not analyze these cases. The purpose of this paper is to show the main features of the equidistant optimization for different limiting fields. If our proposal is taken into service, optimization of the end cells of any shape can be easily done.

Results of optimization of inner cells—maximal achievable accelerating rates for different values of E^*_{pk}/B^*_{pk}—are presented in Fig. 2.

First question that can be asked is the following: What maximal acceleration can be achieved if there is no limitation by magnetic field? Calculations show that the minimal value of E_{pk}/E_{acc} is 1.536 that corresponds to $E^*_{pk}/B^*_{pk} = 100/350$. So, no benefit from increasing the limiting magnetic field above 350 mT can be obtained if the limiting electric field is 100 MV/m. The maximum that can be counted on is about 65 MV/m. For $E^*_{pk} =$ 125 MV/m that can be achieved now with very thorough surface preparation and with $B^*_{pk} = 400$ mT that hopefully can be obtained with a new material, we can recon not more than on 80 MV/m. Further increase of the limiting magnetic field B^*_{pk} above 400 mT will not lead to any increase of the accelerating rate as long as E^*_{pk} remains equal to 125 MV/m.

We examine here the elliptic cavities. However, the optimal cavity for the minimal possible $E_{pk}/E_{acc} = 1.536$ degenerates to a cavity with zero half-axes of the upper ellipse: $A = 0$, $B = 0$.

A row of optimal shapes for different E^*_{pk}/B^*_{pk} is presented in Fig. 3. The vertical line on the right side of each shape is the length of the cavity. For the optimization 200/200, the value of A becomes larger than L, that is, physically impossible for inner cells, here it is just a mathematical result.

Dimensions and field ratios for different values of E^*_{pk}/B^*_{pk} are presented in Table I. The areas corresponding to the colored areas in Fig. 2 are separated by vertical lines.

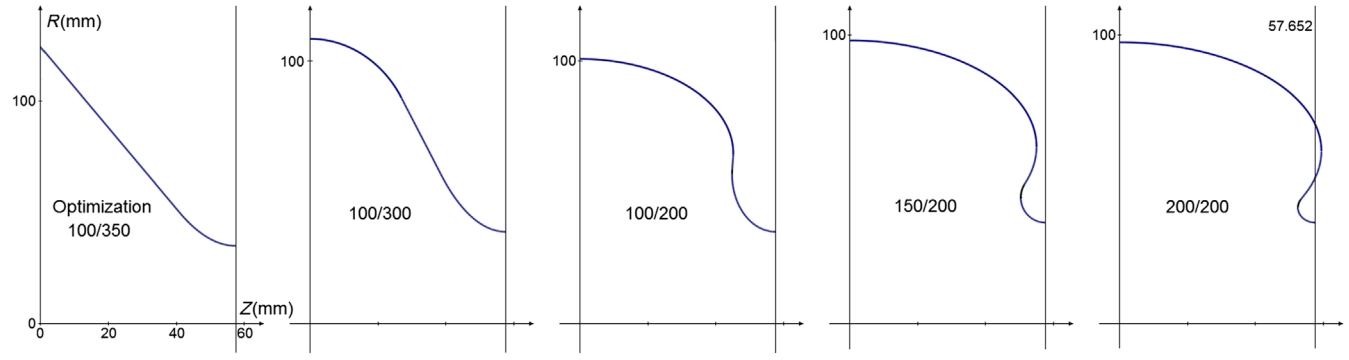

FIG. 3. Optimal shapes of inner cells for different values of E^*_{pk}/B^*_{pk}, aperture radius $R_a = 35$ mm.

TABLE I. Result of equidistant optimization of inner cell of a multicell cavity, aperture radius is 35 mm, frequency is 1300 MHz. Units for B_{pk}/E_{acc} are mT/(MV/m). Vertical lines in the table correspond to boundaries of areas in Fig. 2.

E^*_{pk}/B^*_{pk}, (MV/m)/mT	100/350 (0.286)	100/300 (0.333)	100/250 (0.4)	100/200 (0.5)	127/200 (0.635)	150/200 (0.75)	172/200 (0.862)	200/200 (1)
E_{pk}/E_{acc}	1.536	1.62	1.745	1.998	2.399	2.767		3.605
B_{pk}/E_{acc}	5.43	4.86	4.36	4.00	3.78	3.69		3.60
A, mm	0	31.2	38.5	45.2	51.63	55.06	57.652	59.5
B, mm	0	45.4	38.3	35.9	36.10	36.78		37.65
a, mm	500	35.8	20.1	12.8	9.06	7.23		5.06
b, mm	2726	141.6	48.1	21.8	12.04	8.65		5.15
R_{eq}, mm	124.5	108.417	103.689	100.742	98.707	98.012		97.369
α, deg.	118.8	111.8	98.9	86.8	69.0	61.7		57.5

V. MINIMAL POSSIBLE PEAK ELECTRIC FIELDS FOR DIFFERENT APERTURES

If we have no limitations by the magnetic field, the optimal cavities have a shape like in the first picture in Fig. 3, the minimal value of E_{pk}/E_{acc} depends only on the aperture radius. This dependence is shown in Fig. 4. There is a flat minimum near $R_a = 15$ mm with $E_{pk}/E_{acc} = 1.26$.

A question can be asked is the following: Can it be that this value is less than $\pi/2$, the flight time factor for a pillbox cavity with a zero-aperture radius? The answer is "yes" because in the triangle cavity, the force lines near the metal wall are distributed on the tilted surface near the iris.

VI. HIGH-Q CAVITIES FOR INDUSTRIAL LINACS

Now an industrial linac is under consideration, which is based on Nb_3Sn-coated ILC-type 1.3-GHz acceleration cavity [8,9]. We will present results of optimization for this frequency though lower frequencies are also being considered for industrial linacs: 750 MHz [10], or 650 MHz [11,12]. Our results can be simply scaled to different frequencies. High Q_0 at 4.4 K allows conduction cooling and cryocooler instead of He bath and refrigerator, which is extremely attractive for linacs operating in an industrial environment. However, a standard cryocooler may remove 2–2.5 W at 4.2 K [12], and it is not reasonable to increase the gradient beyond ~8 MeV/m using 2–3 cryocoolers, because of Q_0 drop, see Fig. 11 in [9]. Further increase of the gradient is not reasonable, the loss, say at 10 MeV/m, reaches 12 W/m and the number of cryocoolers is impractical.

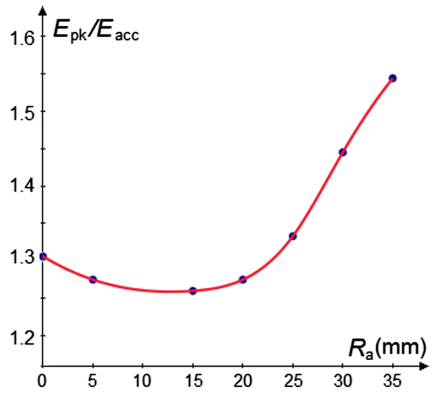

FIG. 4. Minimal possible values of E_{pk}/E_{acc} for different aperture radii.

An increase in gradient has been demonstrated with cryocoolers at a frequency of 915 MHz, up to 12.8–13.6 MV/m [13], but it was done with a single-cell cavity whose optimization is different, see below, and for a low β, the speed of the electron relative to the speed of light.

Returning to the ILC-type structure used in some experiments with cryocoolers, we can note that this structure is optimized for high gradient, not high Q_0: $E_{pk}/E_{acc} = 2$ and $B_{pk}/E_{acc} = 4.26$ mT/(MeV/m). For $E_{acc} \sim 10$ MeV/m, one has a surface electric field of 20 MV/m, it is too low compared to the field emission onset. On the other hand, B_{pk} is too high, 42.6 mT, providing a significant drop in Q_0. It is possible for a production version to reoptimize the linac, completely changing balance between E_{pk} and B_{pk} to smaller values of B_{pk}.

Figure 5 shows that the acceleration rate of 10 MV/m can be achieved at $B_{pk} = 36$ mT. This is more than 15% less than in the case of the TESLA cavity shape and makes cryocooling more practical.

For reentrant cavities, the distance L-A is the distance between the inner surfaces of neighbor cells and should be big enough to account for the thickness of the material and the gap needed to weld the cells together.

Optimization for $E^*_{pk}/B^*_{pk} > 0.5$ (MV/m)/mT will lead to an increase of the half-axis A (Fig. 1) so that starting from the point marked as $\Delta 0$, see Fig. 3, the difference $\Delta = L - A$ can become less than zero when E^*_{pk} is increasing. However, we can make the optimization not increase A above a given value. This is shown in Fig. 5. The lower branch in each of the three groups of curves presents the extreme case when the Δ is limited by zero for $E^*_{pk}/B^*_{pk} > 50/50$ and is shown as a reference, the next

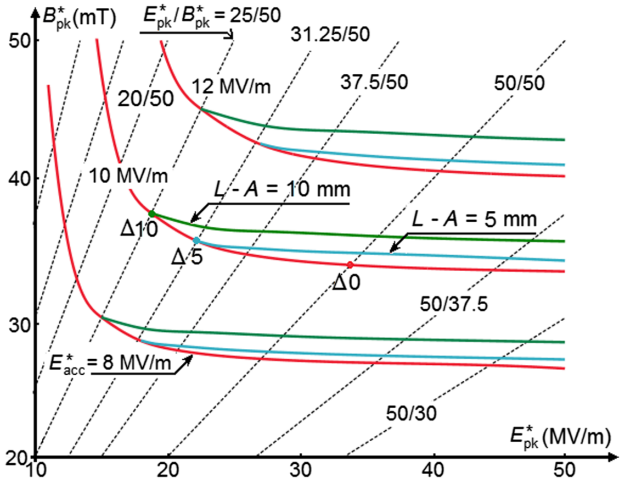

FIG. 5. Equidistant optimization for inner cells of a multicell cavity when the increase in A is limited by certain values. Aperture radius $R_a = 30$ mm.

one marked as Δ5 corresponds to a limitation of 5 mm, and Δ10 is for 10 mm. The points Δ0 and so on are shown on the middle group of curves but are related to all groups because the shape of cells is the same on each dashed line.

In addition to Fig. 5, the results of optimization for low magnetic field cavities are presented in Table II. In the last line of Table II are values of the product $G \times R_{sh}/Q$, where G is the geometry factor, and R_{sh}/Q is the geometric shunt impedance. This product defines losses in the cavity, e.g., for the TESLA cavity $R_{sh}/Q = 15400$ Ohm^2. One can see that losses in the optimized cavities can be up to 30% less than in the TESLA cavity with the same accelerating rate due to a lower surface magnetic field.

VII. EQUIDISTANT OPTIMIZATION OF A SINGLE-CELL CAVITY

A single-cell cavity is often used for testing new materials and presents the version of the inner cell but with beam tubes added. Such a cavity can also be used as a separate accelerating device.

A single-cell cavity with dimensions of an inner cell of a multicell cavity will have values E_{pk}/E_{acc} and B_{pk}/E_{acc} different from those of the inner cell because of different boundary conditions. Now, the length of the half-cell, L, becomes an independent geometric parameter for optimization along with A, B, a, and b.

First of all, let us define, what is E_{acc} for a single cell. The choice of the cavity length, i.e., the distance $2L$ [Fig. 1(b)], should be done so that the acceleration for a given maximal surface field in the cavity is maximal. In the definition of E_{acc} only ΔU, energy gain in volts, is important. So, we should normalize this value of ΔU on the same value $2L_0$ for any geometric parameters: A, B, a, and b, including the distance from the aperture end of the smaller ellipse to the plane of the equator, and find the maximal $E_{acc} = \Delta U/2L_0$ giving maximal ΔU.

Obviously, that $L < L_0$, because if beam pipes are added to a cell with $L = L_0 = \lambda/4$, E_{acc} will decrease: the field propagating into the pipes becomes decelerating when the charged particle is in the pipes. A particle moving close to the speed of light will be accelerated only on the length equal to $\lambda/2$, even if it enters the cavity at a

TABLE II. Geometrical and electromagnetic parameters for Fig. 5. Units for B_{pk}/E_{acc} are mT/(MV/m). If there are two lines in a table cell, they belong to different As (i.e., to different gaps $\Delta = L - A$): The first set is for the upper lines ($\Delta = 5$ mm), and the second set is for the second lines ($\Delta = 10$ mm).

E^*_{pk}/B^*_{pk} (MV/m)/mT	20/50 (0.4)	25/50 (0.5)	31.25/50 (0.625)	37.5/50 (0.75)	50/50 (1)	50/30 (1.667)
E_{pk}/E_{acc}	1.64	1.88	2.22	2.62	3.45	5.64
			2.28	2.72	3.59	5.88
B_{pk}/E_{acc}	4.11	3.76	3.56	3.50	3.45	3.39
			3.65	3.62	3.59	3.54
A, mm	39.45	46.25	52.04	52.65	52.65	52.65
			47.65	47.65	47.65	47.65
B, mm	38.99	38.63	38.52	40.35	41.86	43.17
			38.45	40.69	44.38	45.2
a, mm	19.55	11.9	8.61	9.31	10.35	11.34
			10.46	11.20	13.64	14.7
b, mm	57.18	22.45	12.74	8.91	5.90	2.89
			10.55	7.30	5.73	2.7
α, deg.	98.5	83.6	69.4	65.6	61.6	59.2
			88.6	86.5	72.2	67.3
$G \times R_{sh}/Q$, Ohm^2	16 230	18 000	19 160	19 680	20 220	20 860
			18 770	19 080	19 540	20 150

TABLE III. Results of equidistant optimization "100/200" for the inner cell of a multicell cavity and for the single-cell cavity. $R_a = 35$ mm. Units for B_{pk}/E_{acc} are mT/(MV/m), E_{acc} is in MV/m.

	A, mm	B, mm	a, mm	b, mm	L, mm	E_{pk}/E_{acc}	B_{pk}/E_{acc}	E_{acc}
Inner cell	46.2	40.6	11.8	21.8	57.652	1.88	3.76	53.1
Single cell	25.7	30.17	6.74	18.86	30	1.59	3.18	62.9

nonoptimal phase or the cavity length is not equal to $\lambda/2$. This is another reason why E_{acc} should be defined as $E_{acc} = \Delta U/(2L_0) = \Delta U/(\lambda/2)$.

An example of the difference in optimization of the inner cell of a multicell cavity and of a single-cell cavity is presented in Table III. Here equidistant optimization is done for $E^*_{pk} = 100$ MV/m and $B^*_{pk} = 200$ mT. Note that even having a shorter length L, the single cell has an 18% higher acceleration rate.

VIII. PROCEDURE OF OPTIMIZATION

2D computer code SuperLANS [14] and the TunedCell envelope code [15] have the accuracy needed for our optimization. These codes tune the cell with a given geometry to a needed frequency, changing its equatorial radius, and for the end cells, tuning is done by changing the length L.

The goal function (1) belongs to a class of so-called ravine functions, these functions look like a surface in the ravine: it rapidly grows on the steep shores and slowly declines along the waterway. This property makes it possible to change the geometric parameters in a broad range, but only if they belong to a correct direction, "along the waterway." This property is important to find a shape free of multipactor, not compromising much the goal function, moving along the "bottom" of the ravine. This procedure is described in more detail in [7].

Gradient descent becomes difficult for this class of functions. We used the "brute force," or "grid search" approach to search for a minimum of the goal function on a 4D grid for four variables: A, B, a, and b, with a definite step. The step of the grid can be decreased until we reach the required accuracy. More details about the procedure of optimization can be found in [16].

IX. CONCLUSION

A new method—equidistant optimization—is implemented for standing wave cavities. This method allows to optimize the cavity cell shape for the highest possible accelerating gradient with any values of limiting fields. Two cases are considered: (i) Inner cells of a cavity with a high accelerating rate due to high limiting magnetic fields. It is shown that for expected new materials with a high critical magnetic field, the limitation in accelerating rate comes to the surface electric field. Also, a single-cell cavity optimization is analyzed. (ii) Cavities with a high Q factor at a low magnetic field like in Nb_3Sn. The optimization was also done for the highest gradient but because the magnetic field was limited, we keep the highest Q. These cavities can be used for industrial linacs with cryocooling. The found best shapes can decrease losses up to 30% compared to commonly used cavities at the same accelerating rate or increase this rate at the same losses.

[1] R. L. Geng *et al.*, World record accelerating gradient achieved in a superconducting niobium RF cavity, in *Proceedings of the 21st Particle Accelerator Conference, Knoxville, TN, 2005* (IEEE, Piscataway, NJ, 2005), p. 653.

[2] V. Shemelin, H. Padamsee, and R. L. Geng, Optimal cells for TESLA accelerating structure, Nucl. Instrum. Methods Phys. Res., Sect. A **496**, 1 (2003).

[3] F. Pei-Jen Li and A. Gurevich, Effect of impurities on the superheating field of type-II superconductors, Phys. Rev. B **85**, 054513 (2012).

[4] Danilo B. Liarte, S. Posen, Mark K. Transtrum, G. Catelani, M. Liepe, and James P. Sethna, Theoretical estimates of maximal fields in superconducting resonant radio frequency cavities: stability theory, disorder, and laminates, Supercond. Sci. Technol. **30**, 033002 (2017).

[5] F. Furuta *et al.*, Experimental comparison at KEK of high gradient performance of different single cell superconducting cavity designs, in *Proceedings of the 10th European Particle Accelerator Conference, Edinburgh, Scotland, 2006* (EPS-AG, Edinburgh, Scotland, 2006), p. 750.

[6] R. L. Geng *et al.*, High gradient studies for ILC with single-cell re-entrant shape and elliptical shape cavities made of fine-grain and large-grain niobium, in *Proceedings of the 22nd Particle Accelerator Conference, PAC-2007, Albuquerque, NM* (IEEE, New York, 2007), p. 2337.

[7] V. Shemelin, H. Padamsee, and V. Yakovlev, Optimization of a traveling wave superconducting RF cavity for upgrading the International Linear Collider, Phys. Rev. Accel. Beams **25**, 021001 (2022).

[8] R. Kephart *et al.*, SRF, compact accelerators for industry & society, in *Proceedings of 17th International Conference on RF Superconductivity, SRF'15, Whistler, BC, Canada* (JACoW, Geneva, Switzerland, 2015).

[9] S. Posen, J. Lee, D. N. Seidman, A. Romanenko, B. Tennis, O. S. Melnychuk, and D. A. Sergatskov, Advances in Nb_3Sn superconducting radiofrequency cavities towards first practical accelerator applications, Supercond. Sci. Technol. **34**, 025007 (2021).

[10] G. Ciovati *et al.*, Design of a cw, low-energy, high-power superconducting linac for environmental applications, Phys. Rev. Accel. Beams **21**, 091601 (2018).

[11] R. C. Dhuley, S. Posen, M. I. Geelhoed, O. Prokofiev, and J. C. T. Thangaraj, First demonstration of a cryocooler conduction cooled superconducting radiofrequency cavity operating at practical cw accelerating gradient, Supercond. Sci. Technol. **33**, 06LT01 (2020).

[12] R. C. Dhuley *et al.*, Design of a 10 MeV, 1000 kW average power electron beam accelerator for wastewater treatment applications, Phys. Rev. Accel. Beams **25**, 041601 (2022).

[13] G. Ciovati *et al.*, Development of a prototype superconducting radio-frequency cavity for conduction-cooled accelerators, Phys. Rev. Accel. Beams **26**, 044701 (2023).

[14] D. G. Myakishev and V. P. Yakovlev, The new possibilities of SuperLANS code for evaluation of axisymmetric cavities, in *Proceedings of the Particle Accelerator Conference, Dallas, TX, 1995* (IEEE, New York, 1995).

[15] D. Myakishev, TunedCell, Cornell University, LEPP Report No. SRF/D051007-01, 2005.

[16] V. Shemelin and S. Belomestnykh, *Multipactor in Accelerating Cavities* (Springer, Switzerland, 2020), Chap. 10, pp. 111–118.